

Understanding Hydrogen Atom Transfer: From Bond Strengths to Marcus Theory

JAMES M. MAYER*

Department of Chemistry, Campus Box 351700, University of Washington,
Seattle, Washington 98195-1700, United States

RECEIVED ON JUNE 25, 2010

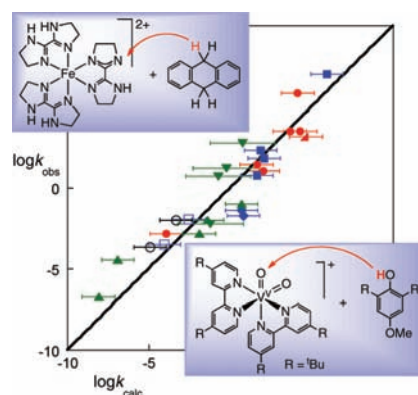
CONSPECTUS

Hydrogen atom transfer (HAT), a key step in many chemical, environmental, and biological processes, is one of the fundamental chemical reactions: $A-H + B \rightarrow A + H-B$. Traditional HAT involves *p*-block radicals such as *tert*-BuO \cdot abstracting H \cdot from organic molecules. More recently, the recognition that transition metal species undergo HAT has led to a broader perspective, with HAT viewed as a type of proton-coupled electron transfer (PCET).

When transition metal complexes oxidize substrates by removing H \cdot ($e^- + H^+$), typically the electron transfers to the metal and the proton to a ligand. Examples with iron-imidazolate, vanadium-oxo, and many other complexes are discussed. Although these complexes may not “look like” main group radicals, they have the same pattern of reactivity. For instance, their HAT rate constants parallel the A–H bond strengths within a series of similar reactions. Like main group radicals, they abstract H \cdot much faster from O–H bonds than from C–H bonds of the same strength, showing that driving force is not the only determinant of reactivity.

This Account describes our development of a conceptual framework for HAT with a Marcus theory approach. In the simplest model, the cross relation uses the self-exchange rate constants ($k_{AH/A}$ for $AH + A$) and the equilibrium constant to predict the rate constant for $AH + B$: $k_{AH/B} = (k_{AH/A}k_{BH/B}K_{eq})^{1/2}$. For a variety of transition metal oxidants, $k_{AH/B}$ is predicted within one or two orders of magnitude with only a few exceptions. For 36 organic reactions of oxyl radicals, $k_{AH/B}$ is predicted with an average deviation of a factor of 3.8, and within a factor of 5 for all but six of the reactions. These reactions involve both O–H or C–H bonds, occur in either water or organic solvents, and occur over a range of 10^{28} in K_{eq} and 10^{13} in $k_{AH/B}$. The treatment of organic reactions includes the well-established kinetic solvent effect on HAT reactions. This is one of a number of secondary effects that the simple cross relation does not include, such as hydrogen tunneling and the involvement of precursor and successor complexes. This Account includes a number of case studies to illustrate these and various other issues.

The success of the cross relation, despite its simplicity, shows that the Marcus approach based on free energies and intrinsic barriers captures much of the essential chemistry of HAT reactions. Among the insights derived from the analysis is that reactions correlate with free energies, not with bond enthalpies. Moreover, the radical character or spin state of an oxidant is not a primary determinant of HAT abstracting ability. The intrinsic barriers for HAT reactions can be understood, at least in part, as Marcus-type inner-sphere reorganization energies. The intrinsic barriers for diverse cross reactions are accurately obtained from the HAT self-exchange rate constants, a remarkable and unprecedented result for any type of chemical reaction other than electron transfer. The Marcus cross relation thus provides a valuable new framework for understanding and predicting HAT reactivity.



I. Introduction

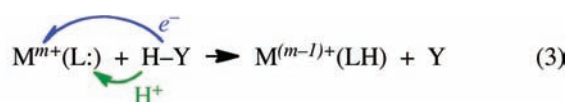
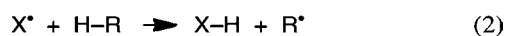
Hydrogen atom transfer (HAT, eq 1) is the most common reaction that involves the transfer of two elementary particles, a proton and an electron.



HAT is a fundamental step in a wide range of processes, from combustion and aerobic oxidations to enzymatic catalysis and the destructive effects of reactive oxygen species in vivo.¹ Organic HAT reac-

tions have been studied for over a century. More recently, metalloenzyme active sites have been shown to oxidize substrates by HAT, which has stimulated explorations of transition metal mediated HAT. This Account describes studies from our laboratory that have allowed us to develop a conceptual framework for all of HAT. We begin with an overview of the reactions and their characteristics, and then develop a model based on Marcus theory that gives quantitative predictions of rate constants and a new understanding of HAT reactions.

Classical organic HAT reactions have an abstracting group that is a p-block radical X^\bullet such as *t*-butoxyl (eq 2). In contrast, transition metal complexes that abstract H^\bullet ($\equiv H^+ + e^-$) typically have an oxidizing metal center to accept the electron and a basic ligand to accept the proton (eq 3).²

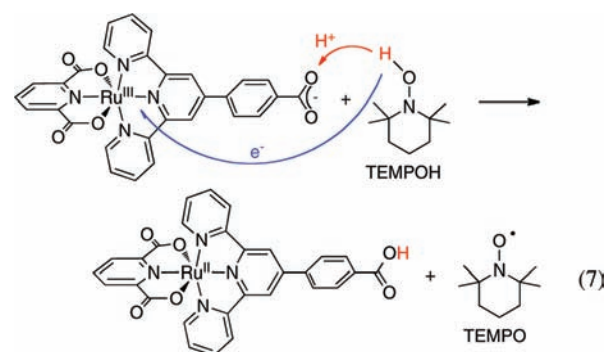
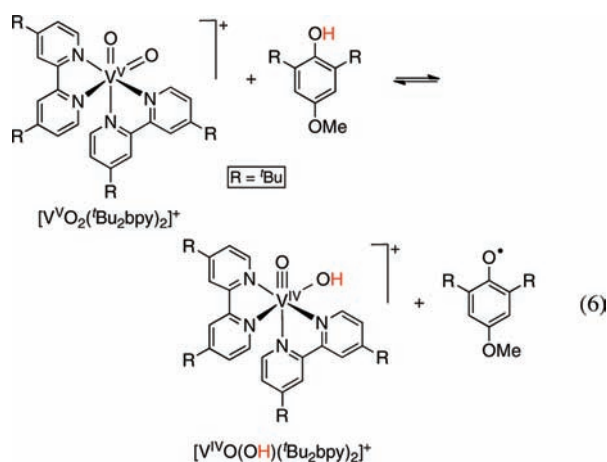
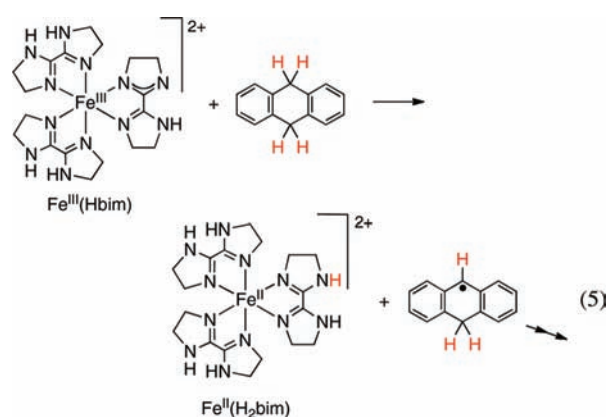
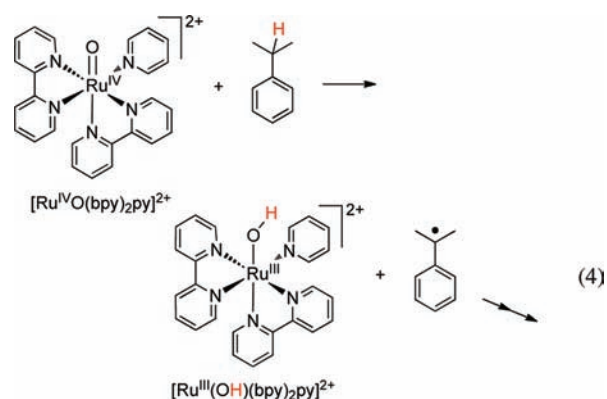


These are sometimes described as proton-coupled electron transfer (PCET) reactions because of the possible separation of the e^- and H^+ .³ Our results show that these disparate-looking reactions are actually very similar. Thus, in our view, the same terminology should be used (HAT) for essentially all reactions in which $H^+ + e^-$ are transferred in one kinetic step from one group to another.

Case Study 1: Examples of Metal-Mediated HAT.

Throughout this Account, we will use “case studies” of particular systems to motivate and illustrate various features of HAT. This first “case” provides four examples of HAT reactions involving metal species (eqs 4–7).^{4–7} The first two are abstractions from C–H bonds and are the first steps in multistep reactions (as indicated by the “ \rightarrow ”). The latter two are abstractions from O–H bonds to form stable oxyl radicals. All of these occur by formal transfer of H^\bullet , with transfer of e^- to the metal and H^+ to a ligand. Thermochemical arguments show that the two particles must transfer in a single kinetic step.^{2,3,8}

In eqs 4 and 6, a metal-oxo group is the abstracting agent, but in eqs 5 and 7 it is not easy to identify a functional group that abstracts H^\bullet . In eq 7, the transferred H^\bullet is separated into the proton that is added to the carboxylate and the electron that is added to the Ru^{III} 11 Å away, and there is very little communication between these sites.⁷ Reaction 7 does not “look like” HAT; it is perhaps more comfortable to describe it as “concerted proton–electron transfer” (CPET).⁹ However, all of these reactions are fundamentally similar to each other and to organic HAT reactions. The large majority of cases have the same pattern of reactivity and are well described by the Marcus theory approach described below.



II. Correlation of HAT Rate Constants with Bond Strengths

In 1938, Evans and Polanyi suggested¹⁰ that, within a set of atom transfer reactions, the log of the rate constants should parallel the reaction energy. Many sets of HAT reactions involving one type of oxidant X^\bullet reacting with various substrates $R-H$ follow this correlation. The differences in reaction energies are usually taken as the differences in the bond dissociation enthalpies (BDEs) of $R-H$ (although free energies should be used; see Case Study 6 below).

Case Study 2: Evans–Polanyi Correlation for HAT to a Ruthenium–Oxo Complex. $[\text{Ru}(\text{O})(\text{bpy})_2\text{py}]^{2+}$ oxidizes $C-H$ bonds in organic compounds by HAT (i.e., eq 4 above). The rate constants for the initial HAT step correlate very well with the $C-H$ BDEs (Figure 1).¹¹ A plot of Eyring barrier versus enthalpic driving force, $\Delta G^\ddagger/\Delta\Delta H^\circ$, has a Brønsted slope $\alpha = 0.47$. A slope of close to 1/2 is predicted by the Marcus treatment below and by most rate/driving force relations for reactions that are not too exo- or endoergic.¹² In such reactions, the transition state usually occurs near the midpoint of the reaction coordinate, following the Hammond postulate, and changes in ΔG° are partially reflected in ΔG^\ddagger . A value of α close to 1/2 is typical of sets of similar HAT reactions with small $|\Delta G^\circ|$.^{1a,11}

II.A. Correlations between Different Oxidants. The Evans–Polanyi analysis can be applied not only to one abstractor with a series of substrates (as is typically done) but also to one substrate with a series of “similar” abstractors. Within organic HAT, it is clear what “similar” means: oxyl radicals are one class, and halogen radicals another. The metal complexes do not look similar to these radicals, so we were surprised when initial studies showed a good $\log k$ versus driving force correlation for oxyl radicals and metal oxidants.¹³ This correlation involved H^\bullet abstraction from dihydroanthracene by ${}^t\text{BuO}^\bullet$, ${}^s\text{BuOO}^\bullet$, $[\text{Ru}(\text{O})(\text{bpy})_2\text{py}]^{2+}$, MnO_4^- , $[\text{Mn}_2(\mu\text{-O})_2(\text{phen})_4]^{3+}$, $[\text{Mn}_2(\mu\text{-O})(\mu\text{-OH})(\text{phen})_4]^{3+}$, and $\text{Fe}^{\text{III}}(\text{Hbim})$. More recently, however, we have found metal complexes that deviate from this correlation (cf. Case Studies 5 and 7 below). These results provided an incentive to explore the Marcus model (section III), to address what makes H-atom abstractors “similar” such that they correlate on the same Evans–Polanyi line.

II.B. Reactivity and Spin State. There is a long-held intuition that H-atom abstractors are radicals, and that radical character at the abstracting atom is critical to HAT. The Evans–Polanyi correlation with different oxidants presented above shows that this intuition is incorrect. The correlation

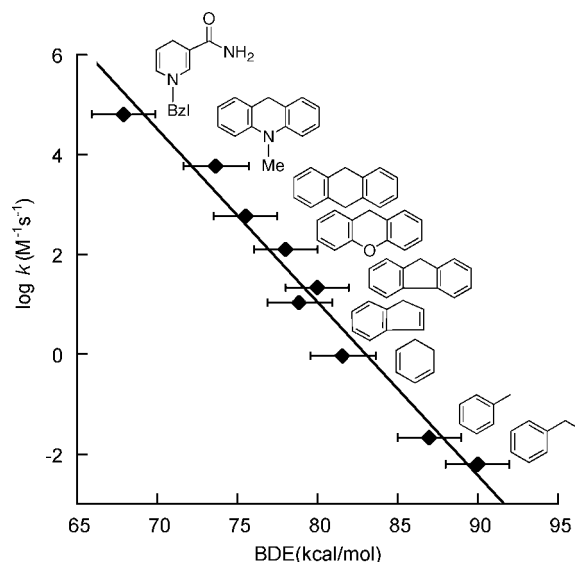
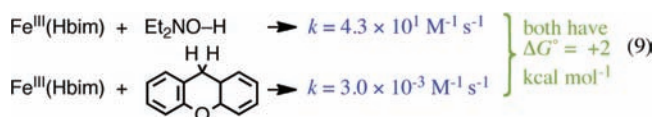
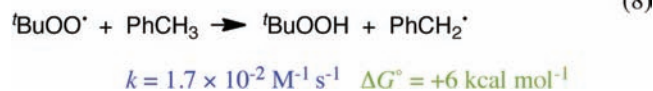
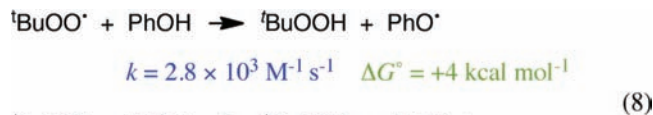


FIGURE 1. Plot of rate constants (statistically corrected) for HAT from alkylaromatic compounds to $[\text{Ru}(\text{O})(\text{bpy})_2\text{py}]^{2+}$.¹¹

includes oxyl radicals with doublet spin states, an $S = 5/2$ iron(III) complex, antiferromagnetically coupled manganese dimers (with both integer and half-integer spin states), and diamagnetic (d^0) permanganate. There are other examples of H-atom abstractors that have no unpaired spins, or no apparent spin density at the abstracting atom, including d^0 Cr^{VI} compounds,¹³ the ruthenium complex in eq 7, and even (in the elegant work by Rüchert et al.) organic compounds such as α -methylstyrene.¹⁴ Conversely, O_2 and the nitroxyl radical TEMPO are very poor H-atom abstractors despite their unpaired spins. *The presence of unpaired spin density at the abstracting atom is not a requirement for, or a predictor of, HAT reactivity.*

Case Study 3: Reactions of O–H versus C–H Bonds. It has long been known that O–H bonds undergo HAT more quickly than C–H bonds of equal strength, so these substrates fall on different Evans–Polanyi correlation lines.^{1,15} A classic comparison is that ${}^t\text{BuOO}^\bullet$ abstracts $H^\bullet \sim 10^5$ faster from phenol than from toluene (eq 8). Their small difference in their BDEs (PhOH , 88.0; PhCH_3 , 89.8 kcal mol^{-1})⁸ accounts for only one of this five-order-of-magnitude difference in k . The same $\sim 10^4$ intrinsic difference in k is seen for $\text{Fe}^{\text{III}}(\text{Hbim})$ abstracting H^\bullet from diethylhydroxylamine versus xanthene, which have equal $Y-H$ bond strengths (eq 9).^{8,13,16} Another example of the similar reactivity of organic radicals and transition metal complexes is that both are remarkably unreactive with acetonitrile,¹⁷ even though the $H-CH_2\text{CN}$ bond is relatively weak. *These comparisons show that bond strengths are not the*

only determinant of HAT reactivity. We will return to the greater kinetic facility of O–H versus C–H bonds in section IV.A below.



III. Introduction to Marcus Theory and the Cross Relation

Marcus–Hush theory and its extensions have been remarkably successful in understanding a wide range of electron transfer (ET) processes.¹⁸ The simplest (adiabatic) form of the Marcus equation (eq 10) predicts the reaction barrier (ΔG^\ddagger) from the reaction driving force (ΔG°) and the intrinsic barrier (λ). λ is the energy required to reorganize the reactants and their surrounding solvent to the structure of the product without the electron transferring, so it is often called the reorganization energy. With a few additional assumptions, the Marcus equation can be rearranged to the Marcus cross relation, eq 11.¹⁸ We were attracted to this approach because all of the parameters are independently measurable. This contrasts with the Evans–Polanyi correlation and related linear free energy relations (LFERs), where the parameters are defined only within the context of the LFER. In addition, the cross relation had been successfully applied to limited sets of other atom and group transfer reactions, although not to HAT.¹⁹ There is, however, not much theoretical basis for using eq 11 for reactions other than ET.²⁰ We have therefore been surprised to find that the cross relation holds very well for a wide range of HAT reactions, with only a few outliers.

$$\Delta G^\ddagger = \frac{(\Delta G^\circ + \lambda)^2}{4\lambda} \quad (10)$$

$$k_{\text{AH/B}} = \sqrt{k_{\text{AH/A}} k_{\text{BH/B}} k_{\text{eq}}} f \quad (11)$$

The cross relation, as applied to HAT, predicts the rate constant for a cross reaction $k_{\text{AH/B}}$ (eq 1). The purely kinetic information is predominantly in the two rate constants for the respective hydrogen-atom self-exchange reactions, one of which is shown in eq 12. The equilibrium constant K_{eq} derives from the ΔG° in eq 10 and is analogous to the driving force in the Evans–Polanyi correlation. The factor f is close to 1 for

many of the reactions discussed here, when $|\Delta G^\circ| \ll 2\lambda$.¹⁸ In this limit and within a series of reactions with similar self-exchange rate constants, $k_{\text{AH/B}}$ varies with the square root of $K_{\text{AH/B}}$ (Brønsted $\alpha = 1/2$).



IV. HAT Self-Exchange Reactions

Case Study 4: HAT Self-Exchange between Ru^{II}(py-imH)(acac)₂ and Ru^{III}(py-im)(acac)₂. Self-exchange rate constants play a central role in the cross relation, so we have measured them in a number of systems. The rate of HAT self-exchange between Ru^{II}(py-imH)(acac)₂ and Ru^{III}(py-im)(acac)₂ was determined by ¹H NMR, observing the broadening of the resonances of the diamagnetic Ru^{II} complex upon addition of increasing amounts of the paramagnetic oxidized form (Figure 2).²¹ The derived $k_{\text{Ru(py-imH)}}$ of $(3.2 \pm 0.3) \times 10^5 \text{ M}^{-1} \text{ s}^{-1}$ is in the range that is convenient to study by this technique (ca. 10^2 – $10^6 \text{ M}^{-1} \text{ s}^{-1}$).

IV.A. Magnitudes of $k_{\text{AH/A}}$. We have found similar values of self-exchange rate constants for the Fe(Hbim) and Ru=O complexes in eqs 4 and 5, $(5.8 \pm 0.6) \times 10^3$ and $\sim 8 \times 10^4 \text{ M}^{-1} \text{ s}^{-1}$, respectively.^{4,28} Estimates of $k_{\text{AH/A}}$ for ^tBuO[•] ($\sim 3 \times 10^4 \text{ M}^{-1} \text{ s}^{-1}$)²² and ^tBuOO[•] ($5 \times 10^2 \text{ M}^{-1} \text{ s}^{-1}$)²³ have been derived from pseudo-self-exchange reactions, such as ^tBuOO[•] + ^sBuOOH. These four reagents have $\log(k_{\text{AH/A}}) = 3.8 \pm 1.1$. Thus, to address the issue raised above, *the key similarity of these reagents (what makes them lie on the same Polanyi correlation line) is their self-exchange rate constant*. In contrast, H-transfer from a C–H bond to a carbon radical is dramatically slower: $k(\text{PhCH}_2^\bullet + \text{PhCH}_3) = \sim 4 \times 10^{-5} \text{ M}^{-1} \text{ s}^{-1}$.²⁴ This $k_{\text{AH/A}}$ is $\sim 10^8$ slower than those for the RO–H + OR reactions above.² This difference of $\sim 10^8$ and the dependence in the cross relation correctly predicts the $\sim 10^4$ higher rate constants for O–H versus C–H bonds at the same driving force (eqs 8, 9 above). The reasons for the greater kinetic facility of O–H bonds have been discussed, but no simple picture has emerged; we note here only the striking similarity with proton transfer reactions ($k_{\text{OH/O}} \gg k_{\text{CH/C}}$) and the lack of dependence on the X–H bond strengths.^{2,25}

Case Study 5: Large Reorganization Energy for a Vanadium–Oxo/Hydroxo Self-Exchange Reaction. With the emerging collection of self-exchange rate constants of $\sim 10^4 \text{ M}^{-1} \text{ s}^{-1}$ for reactions of O–H and N–H bonds, we were surprised to find that vanadium oxo/hydroxo complexes have a $k_{\text{AH/A}}$ that is a million times slower.⁴ The reaction is too slow to measure by ¹H NMR line broadening, so we studied a pseudo-self-exchange reaction using substituted bipyridine ligands,

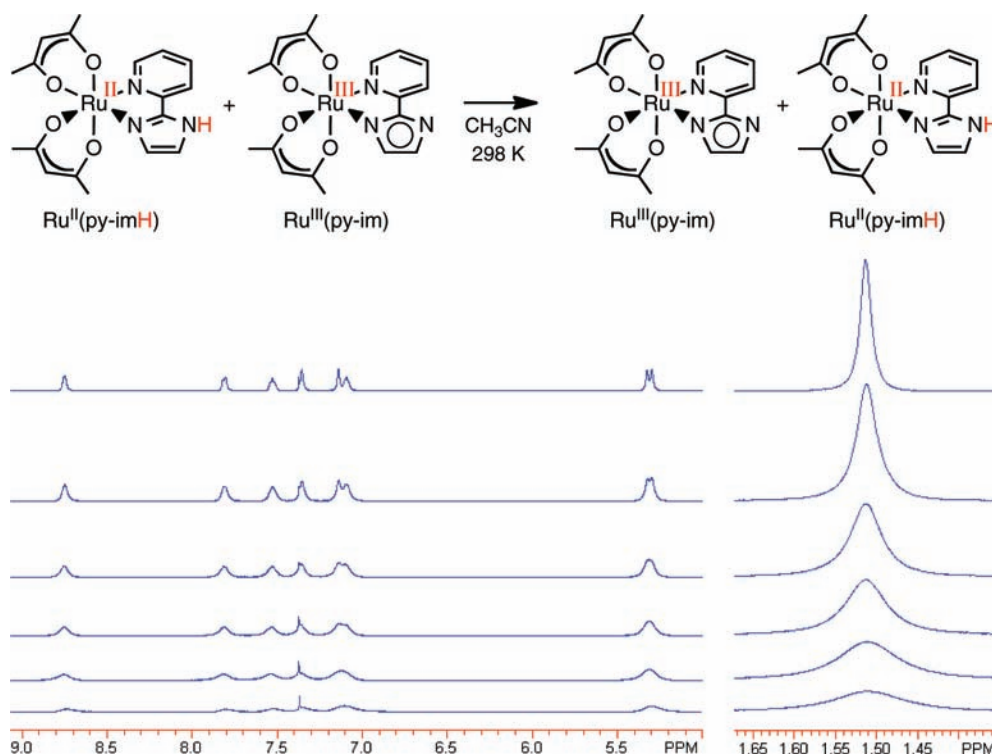


FIGURE 2. Stack plot of ^1H NMR spectra (in CD_3CN) of $\text{Ru}^{\text{II}}(\text{py-imH})(\text{acac})_2$ (top) with increasing amounts of added $\text{Ru}^{\text{III}}(\text{py-im})(\text{acac})_2$.²¹

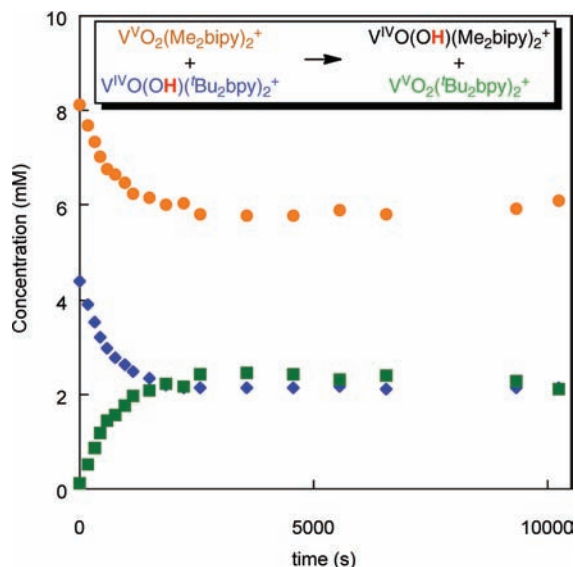


FIGURE 3. Concentration versus time for the reaction of $[\text{V}^{\text{IV}}\text{O}(\text{OH})(\text{Bu}_2\text{bpy})_2]^+$ and $[\text{V}^{\text{V}}(\text{O})_2(\text{Me}_2\text{bpy})_2]^+$ in CD_3CN , monitored by ^1H NMR.

$[\text{V}^{\text{IV}}\text{O}(\text{OH})(\text{Bu}_2\text{bpy})_2]^+ + [\text{V}^{\text{V}}(\text{O})_2(\text{Me}_2\text{bpy})_2]^+$. Three of the four species present in the reaction could be monitored by ^1H NMR, and the approach to equilibrium is shown in Figure 3.

The very slow self-exchange rate constant of $1.3 \times 10^{-2} \text{ M}^{-1} \text{ s}^{-1}$ for $[\text{V}^{\text{IV}}\text{O}(\text{OH})(\text{Bu}_2\text{bpy})_2]^+$ is remarkable, particularly in comparison to that of the related ruthenium complex $[\text{Ru}^{\text{III}}(\text{OH})(\text{bpy})_2\text{py}]^{2+}$, $\sim 8 \times 10^4 \text{ M}^{-1} \text{ s}^{-1}$.^{4a,6} Both reactions involve HAT from MOH to $\text{M}=\text{O}$, and both have bis(bipyridine) supporting ligands. The ruthenium complexes have a higher charge and are more sterically encumbered, yet react $\sim 6 \times 10^6$ times faster. The origin of this contrast was uncovered computationally, comparing $[\text{VO}(\text{O}/\text{H})(\text{bpy})_2]^+$ with $[\text{Ru}(\text{O}/\text{H})(\text{X})(\text{bpy})_2]^+$ ($\text{X} = \text{fluoride}$ or pyrrolate , to compare compounds of equal charge).⁶ As described in Figure 4, the passage from the hydrogen-bonded $\text{MOH} \cdots \text{OM}$ “precursor complex” to the transition structure was divided into three steps for each reaction. The higher barrier in the V system is due to the energy required to change the V–O and V–N bonds from their lengths in the precursor complex to their lengths in the transition structure (step b \rightarrow c). In particular, the $\text{V}^{\text{IV}}\text{–OH}$ single bond becomes a much shorter vanadium(V)-oxo bond with a bond order of 2.5. In the Marcus theory of electron transfer, such a large change in a strong bond would be a classic example of a large inner-sphere reorganization energy, λ_i . Thus, the conceptual picture of λ_i from ET carries over to the intrinsic barriers of metal-mediated HAT reactions.

IV.B. Spin and HAT Intrinsic Barriers. The hydrogen abstracting agent in the case above, $d^0 [\text{V}^{\text{V}}\text{O}_2(\text{bpy})_2]^+$, has no unpaired electrons. Its self-exchange reaction can be written schematically as $\text{V}=\text{O} + \text{HOV}^\bullet$. It therefore does not resemble a typical organic HAT reaction $\text{R}^\bullet + \text{H–R}$, where the radical center and H-atom are on different molecules. Instead, $\text{V}=\text{O} + \text{HOV}^\bullet$ is similar to the reaction of a ketone with a ketyl radical, $\text{R}_2\text{C}=\text{O} + \text{H–O}\dot{\text{C}}\text{R}_2$. However, this “opposite” electronic

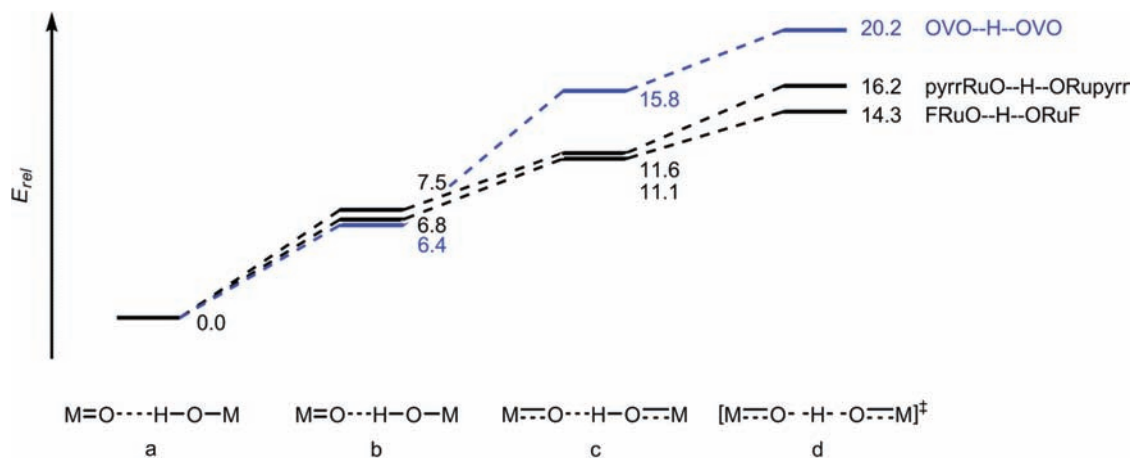


FIGURE 4. Relative gas-phase electronic energies ($\Delta E/\text{kcal mol}^{-1}$), for $[(\text{bpy})_2\text{V}^{\text{VO}}_2]^+ + [(\text{bpy})_2\text{V}^{\text{VO}}(\text{OH})]^+$, for $[(\text{bpy})_2(\text{pyrr})\text{Ru}^{\text{VO}}]^+ + [(\text{bpy})_2(\text{pyrr})\text{Ru}^{\text{III}}(\text{OH})]^+$, and for $[(\text{bpy})_2(\text{F})\text{Ru}^{\text{VO}}]^+ + [(\text{bpy})_2(\text{F})\text{Ru}^{\text{III}}(\text{OH})]^+$, of (a) the optimized hydrogen bonded precursor complexes ($E = 0$); (b) the O...O distances constrained to those in the transition structures, with all other geometrical parameters optimized; (c) all of the atoms moved to their positions in the transition structures, except for the transferring proton, whose position was optimized; and (d) the optimized transition structures.

structure does not appear to affect the rate of HAT: ketyl-radical/ketone reactions occur at $(3.7\text{--}8.6) \times 10^3 \text{ M}^{-1} \text{ s}^{-1}$,²⁶ typical of $\text{RO}^\bullet + \text{H--OR}$ reactions. Large self-exchange rate constants are estimated for MnO_4^- ($\sim 2 \times 10^6 \text{ M}^{-1} \text{ s}^{-1}$) and for CrO_2Cl_2 ($\sim 2 \times 10^3 \text{ M}^{-1} \text{ s}^{-1}$) using the cross relation, even though they are also (d^0) $\text{M}=\text{O} + (d^1)$ HOM^\bullet reactions.⁴ The vanadium system has slow HAT not because of its electronic structure but because of its high reorganization energy.

These data confirm the conclusion above that “radical character” at the abstracting atom is not a primary determinant of HAT reactivity. Spin states can, however, play an indirect role, as molecules in different spin states have different free energies, intrinsic barriers, and activation barriers for HAT. This is perhaps most evident in Shaik’s two-state reactivity model for reactions of first-row metal-oxo species.²⁷ Our laboratory found an example in the HAT self-exchange reaction $\text{Fe}^{\text{II}}(\text{H}_2\text{bip}) + \text{Fe}^{\text{III}}(\text{Hbip})$, both of which are present in solution as mixtures of high-spin and low-spin forms (see eq 13 for compound drawings).²⁸ $k_{\text{AH/A}}$ is slightly faster at lower temperatures, where the low-spin forms are more prevalent. The low-spin forms have lower HAT intrinsic barriers, opposite to the common intuition, because they have smaller changes in Fe–N bond lengths than their high-spin counterparts. In a very interesting recent example, Que et al. have suggested that the much higher reactivity of an $S = 2$ di-iron oxo species versus an $S = 1$ is in part due to its higher spin state.²⁹ In our view, given the success of the Marcus model as described in the next two sections, these differences in reactivity are likely not a direct effect of the spin, but are rather indirect effects resulting from differences in $\Delta G^\circ_{\text{HAT}}$ and/or λ_{HAT} between the spin isomers.

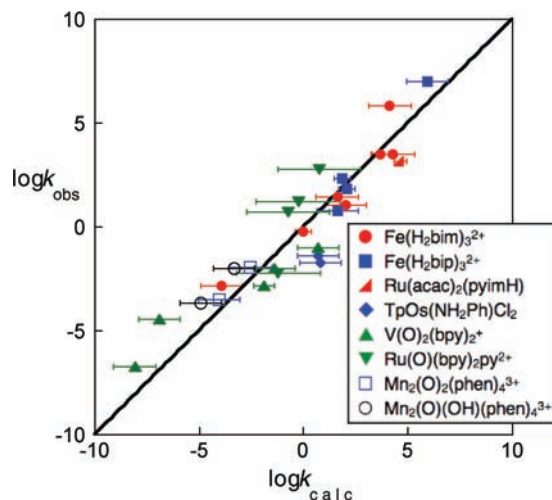


FIGURE 5. Tests of the Marcus cross relation for HAT: log/log plot of observed versus calculated HAT rate constant for a number of metal complexes reacting with various substrates. The diagonal line illustrates $k_{\text{obs}} = k_{\text{calc}}$. The estimated errors on k_{calc} are typically ± 1 log unit; they are larger for MeCN reactions of $\text{Ru}(\text{O})\text{bpy}_2\text{py}^{2+}$ because the BDFE is only available in H_2O , and smaller in three cases where $k_{\text{AH/B}}$ was measured directly.

V. Tests of the Cross Relation for HAT: Metal Complexes

In 2001, we had sufficient data in hand to show that the cross relation predicts HAT reaction rate constants quite well for a variety of reactions.¹⁶ An updated summary of all of our tests of the cross relation with transition metal systems is shown in Figure 5, as a plot of observed versus calculated cross rate constants. The diagonal line indicates what would be perfect agreement. In each case, $k_{\text{AH/B}}$, $k_{\text{AH/A}}$, $k_{\text{BH/B}}$, and $k_{\text{AH/B}}$ are all available from independent measurements. The measured cross rate constants are known to high accuracy on this scale,

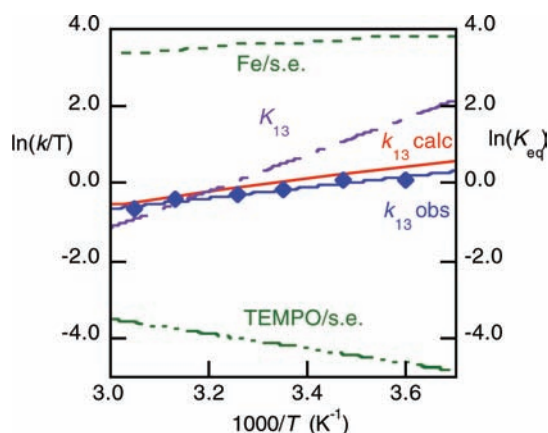
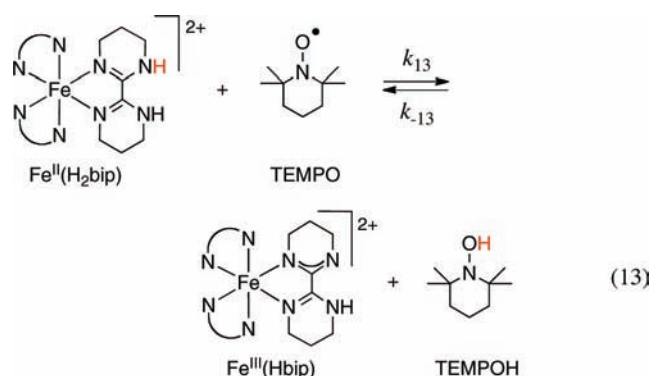


FIGURE 6. Combined Eyring and van't Hoff plot for reaction 13: self-exchange rate constants Fe/s.e. and TEMPO/s.e. (left axis), K_{13} (right axis), and the rate constants measured ($k_{13\text{obs}}$, blue diamonds) and calculated from the cross relation ($k_{13\text{calc}}$, red line) (left axis).³⁰

but most of the calculated values have significant uncertainties due to the limited accuracy of $K_{\text{AH/B}}$. While some reactions deviate from the predictions, the cross relation captures the general sweep of the HAT rate constants over the range of almost 10^{14} in $k_{\text{AH/B}}$. The generally good agreement over such a wide range of reactions, involving different metals, spin states, and O–H, N–H, and C–H bonds is remarkable, especially since this analysis does not include important factors such as solvent effects and precursor complexes (as discussed in section VI and Case Study 6).

Case Study 6: The Cross Relation Predicts and Explains an Unusual Temperature Dependence; the Importance of Using Free Energies. HAT from $\text{Fe}^{\text{II}}(\text{H}_2\text{bip})$ to the stable nitroxyl radical TEMPO (eq 13) is very unusual in that it becomes faster at lower temperatures, with $\Delta H^\ddagger = -2.7 \pm 0.4 \text{ kcal mol}^{-1}$.³⁰ We measured the rates in both directions, determined K_{13} from both kinetic and static measurements, and measured the self-exchange rate constants, all from 277 to 328 K. Together, these allowed an application of the cross relation over a range of temperatures. As shown in Figure 6, the cross relation quantitatively predicts the cross rate constants and the negative temperature dependence ($\Delta H^\ddagger_{\text{calc}} = -3.5 \pm 0.5 \text{ kcal mol}^{-1}$).³⁰ The cross relation not only predicts the rate constants, it also shows *why* reaction 13 becomes faster at low temperatures. The most temperature dependent parameter in the analysis is the equilibrium constant. The reaction is thermodynamically more favorable at low temperatures, and this is the primary contributor to the temperature dependence of k_{13} . Marcus and Sutin analyzed a related situation in 1975, for an ET reaction with $\Delta H^\ddagger < 0$.³¹ This reaction thus shows both the applicability and the value of the cross relation for HAT.



$\text{Fe}^{\text{II}}(\text{H}_2\text{bip}) + \text{TEMPO}$ (eq 13) is a very unusual HAT reaction because it has a substantial ground state entropy change: $\Delta S^\circ_{13} = -30 \pm 2 \text{ cal mol}^{-1} \text{ K}^{-1}$ (from both van't Hoff and calorimetric measurements).^{32,33} HAT reactions typically have $|\Delta S^\circ| \approx 0$ because there is no change in the charges of the species involved and little change in their sizes. The unusual large $|\Delta S^\circ_{13}|$ is primarily a result of vibrational entropy differences between the Fe^{II} and Fe^{III} complexes,³² and it means that ΔH°_{13} is very different from ΔG°_{13} . The close agreement in Figure 6 requires use of free energies (K_{13}); if ΔH were used, $k_{13\text{calc}}$ would deviate by a factor of $\sim 10^3$ at 298 K.

This example shows that analyses of HAT rate constants should use free energies, despite the widespread Polanyi correlations with ΔH° . In fact, Evans and Polanyi's 1938 analysis was in terms of ΔG° , but made the simplifying assumption that $\log(K_{\text{eq}})$ "varies approximately in proportion to the reaction heat."¹⁰ For most organic HAT processes, $|\Delta S^\circ| \approx 0$ and $\Delta H^\circ \approx \Delta G^\circ$, so this distinction is not significant. However, HAT reactions of high-spin transition metal complexes often have large entropy changes,³³ and free energies must be used. More generally, given the importance of linear free energy relationships in reaction chemistry, we encourage practitioners to switch from bond dissociation enthalpies (BDEs) to bond dissociation free energies (BDFEs).⁸

Case Study 7: Precursor and Successor Complexes, and Spin-Forbidden HAT Involving Cobalt Complexes. The application of Marcus theory to bimolecular reactions assumes that the reactants diffuse together to form a precursor complex (PC), which undergoes reaction to form a successor complex (SC) that dissociates to products.¹⁸ In ET reactions, the PC and SC are nonspecifically associated and the often significant energies to form these complexes can be estimated by simple electrostatic models.¹⁸ In HAT reactions, however, electrostatic contributions are typically small because no net charge is transferred and often one of the

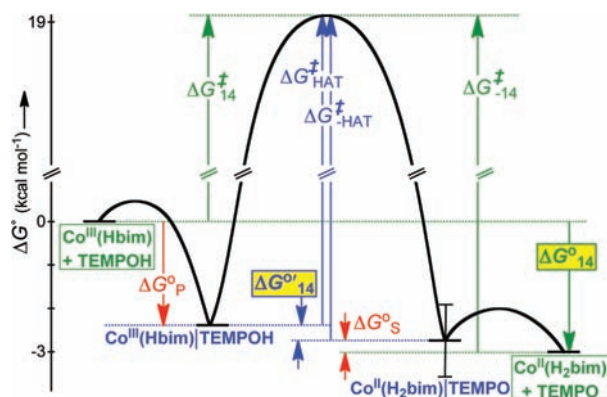
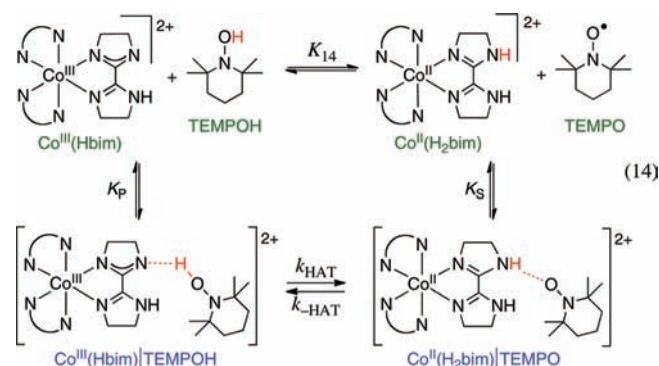


FIGURE 7. Schematic free energy surface for the reaction 14.³⁵

reactants is neutral. More significantly, PCs for HAT reactions must have specific orientations because the proton transfers only over a very short distance. When H⁺ transfers between electronegative elements, the HAT precursor complex most likely involves a hydrogen bond. Even in reactions of C–H bonds where hydrogen bonding should be minor, steric effects can play a major role.³⁴

HAT from TEMPOH to Co^{III}(Hbim) (Figure 7) is a case where the energetics of precursor and successor complexes are significant.³⁵ A scheme showing the precursor and successor complexes in the reaction of Co^{III}(Hbim) with TEMPOH is presented as eq 14. The forward reaction exhibits saturation kinetics at high [TEMPOH], indicating the pre-equilibrium formation of an intermediate, which was identified as a weakly hydrogen bonded PC ($K_p = 61.3 \pm 0.8 \text{ M}^{-1}$). No saturation is observed in the reverse direction ($0.16 < K_s < 2.6 \text{ M}^{-1}$). Incorporating these values into a schematic free energy surface (Figure 7) shows that while the overall reaction has $\Delta G^\circ_{14} = -3.0 \pm 0.4 \text{ kcal mol}^{-1}$, the actual unimolecular HAT step has $\Delta G^\circ_{14} = -0.3 \pm 0.9 \text{ kcal mol}^{-1}$. (The ΔG° terminology follows that used in the ET literature.¹⁸) The $2.7 \pm 1.0 \text{ kcal mol}^{-1}$ difference between ΔG°_{14} and $\Delta G^\circ'_{14}$ corresponds to a difference of about 2 orders of magnitude in $K_{\text{AH/B}}$ and 1 order of magnitude in the predicted rate constant. In the applications of the cross relation summarized in Figure 5 above, the energetics of the PC and SC were not known and were therefore not included in the analyses. This can introduce uncertainty into the calculated cross rate constant, particularly when the hydrogen bonding is different in the PC and SC. This is therefore a limitation in the analysis.

The reaction of Co^{III}(Hbim) with TEMPOH is also interesting because it is formally spin-forbidden. Both Co^{III}(Hbim) and TEMPOH are diamagnetic, so the reactant state is $S = 0$. The cobalt product Co^{II}(H₂bim) is $S = 3/2$ (high-spin d^7) so its com-

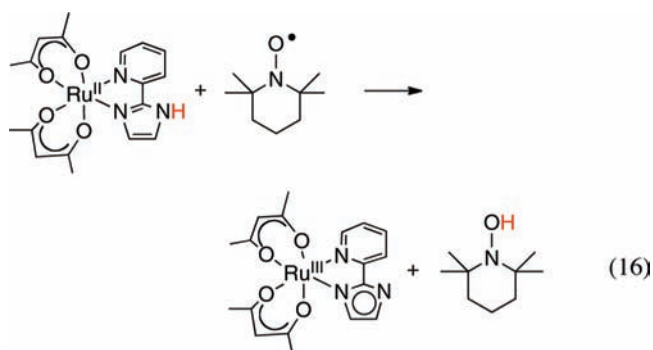
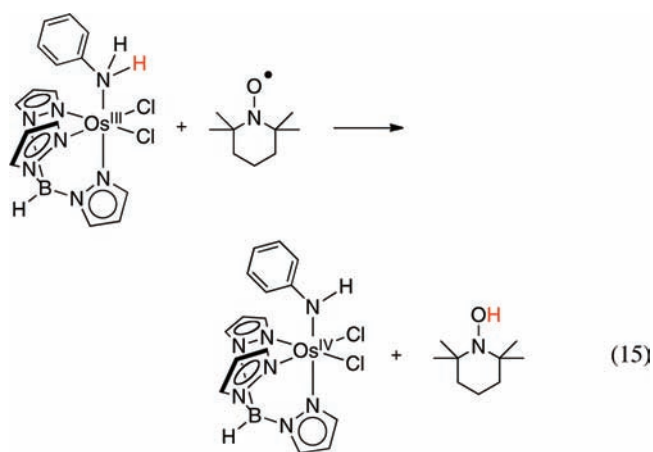


ination with the $S = 1/2$ TEMPO radical can give $S = 1$ or $S = 2$ product states. While there have been many discussions of the relevance of the spin state of the oxidant on HAT, this is to our knowledge the first clear example of a spin-forbidden HAT reaction. This spin issue, and the large difference in Co–N distances between low-spin Co^{III}(Hbim) and high-spin Co^{II}(H₂bim) (large λ_{HAT}), are probably the reasons for the cobalt reaction being very slow. For instance, HAT from Co^{II}H₂bim to TEMPO is more than 10^6 times slower than the related HAT from the iron complex Fe^{II}(H₂bip) to TEMPO (eq 13).³⁰ The iron reaction is $\sim 2.7 \text{ kcal mol}^{-1}$ more favorable, but this likely accounts for only a factor of 10 difference in the rate constants.

Case Study 8: Osmium and Ruthenium Reactions That Show Poorer Agreement with the Cross Relation.

The osmium–aniline complex shown in eq 15 slowly transfers H[•] to the nitroxyl radical TEMPO [$k_{15} = (4 \pm 1) \times 10^{-2} \text{ M}^{-1} \text{ s}^{-1}$].³⁶ This is 80 times slower than the value predicted by the cross relation. (The original report gave the discrepancy as 300 \times , but it is recalculated here using our new measurement of $k_{\text{TEMPOH/TEMPO}}$ in MeCN rather than a literature value in CCl₄.³⁷) The reason for this deviation is not known, although it could arise from the substantial steric crowding in both the cross and self-exchange reactions, or from difficulties in estimating the osmium self-exchange rate constant. In this system, ET and PT self-exchanges are much more facile than HAT self-exchange, and therefore, the HAT reactions were plagued with catalysis by trace acids, bases, oxidants, and reductants.³⁶ Still, the very low self-exchange rate constant [$(3 \pm 2) \times 10^{-3} \text{ M}^{-1} \text{ s}^{-1}$] is qualitatively consistent with the low cross rate constants.

The Ru^{II}(py-imH)+TEMPO reaction (eq 16) has a H/D kinetic isotope effect (KIE) of 23 ± 3 at 298 K, and the temperature dependence of this KIE indicates a significant contribution from proton tunneling.²¹ Surprisingly, the ruthenium self-exchange reaction (Figure 2 above²¹) has a KIE of only 1.5 ± 0.2 ,²¹ while the TEMPO/H reaction (estimated from a pseudo-



self-exchange reaction) has a KIE of 23.³⁷ Large KIEs are frequently observed in metal-mediated HAT reactions, but there is little intuitive understanding of why a particular system might give a large value while another does not. Semiclassical tunneling models emphasize the role of barrier height and width, while recent theoretical treatments of PCET provide a more detailed view and suggest that most H-transfers involve significant tunneling.³⁸

Using these rate constants, the cross relation predicts k_{16H} and k_{16D} that are 31 ± 4 and 140 ± 20 times, respectively, faster than those observed. The predictions are relatively precise because K_{16} was measured directly.²¹ The cross relation is essentially a classical model, so it is not surprising that there could be significant deviations when tunneling contributes substantially to the rates.

VI. More Tests of the Cross Relation: Organic Reactions of Oxyl Radicals and Solvent Effects

HAT reactions of oxyl radicals and hydroxyl compounds are important in processes from autoxidations to aging. Ingold, Litwinienko, and co-workers have shown that abstractions from RO–H bonds are very solvent dependent while abstractions from C–H bonds are not.³⁹ This is because hydrogen-bonded species ROH···solvent are unreactive toward HAT; they must

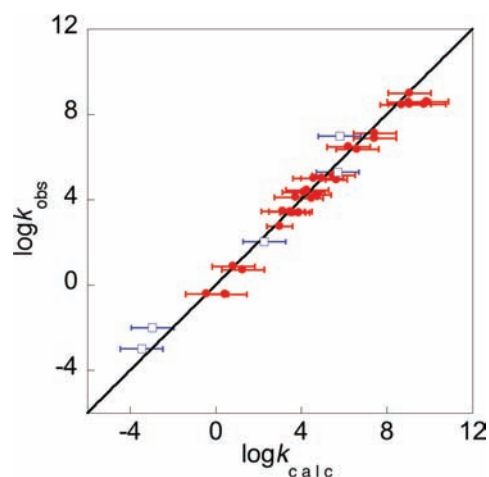


FIGURE 8. Comparison between HAT rate constants measured experimentally (k_{obs}) versus those determined from the CR/KSE model (k_{calc}), involving oxyl radicals + O–H bonds (●) or C–H bonds (□).⁴¹ The line indicates perfect agreement.

dissociate the solvent prior to reaction. The Ingold kinetic solvent effect (KSE) model quantitatively predicts HAT rate constants as a function of solvent, by estimating H-bond equilibrium constants using Abraham's empirical parameters.⁴⁰ This model is separate from the precursor/successor complexes discussed above, because ROH···solvent must dissociate prior to forming the precursor complex.

We have combined the cross relation, the KSE approach, and Abraham parameters to give a CR/KSE model that can predict HAT rate constants using equilibrium constants and self-exchange rate constants from different solvents.⁴¹ The KSE model and Abraham parameters are used to obtain equilibrium and rate constants in a given solvent, which are then used in the cross relation. This model has been tested for 36 organic reactions involving RO• abstracting from O–H or C–H bonds, in water or organic solvents. The reactions range from 2,4,6-*t*-Bu₃C₆H₂O• + TEMPOH to *t*BuOO• + PhCH₃, and span a range of 10²⁸ in K_{eq} and 10¹² in $k_{\text{AH/B}}$. As shown in Figure 8, the agreement is excellent. The overall correlation coefficient is 0.97, and the average deviation is a factor of 3.8. For all but 6 of the 36 reactions, the deviation is less than a factor of 5.

VII. Conclusions: Insights, Oversights, and Questions from the Marcus Analysis

The success of the cross relation in predicting HAT rate constants (Figures 5, 6, and 8) is remarkable and informative. Typically, linear free energy relationships hold only over a narrow set of similar reactions, but the cross relation accurately predicts rate constants for the large majority of organic and transition metal HAT reactions, including substrates with C–H, N–H, and O–H bonds and in solvents from water to hydro-

carbons. The reactions cover huge ranges of driving forces and rate constants.

The most remarkable aspect of this agreement is that HAT intrinsic barriers can be independently determined from self-exchange reactions. This derives from the “additivity postulate” that λ for the cross reaction is the mean of the self-exchange λ 's. For outer-sphere ET reactions, the additivity postulate is intuitively reasonable because no chemical bonds are made or broken and the precursor and successor complexes are nonspecifically associated.¹⁸ However, this is quite surprising for HAT reactions. In reactions of RO[•] with C–H bonds, for instance, the transition structure of one of the self-exchange reactions is stabilized by a hydrogen bond (ROH \cdots OR),⁴² but those for the other self-exchange reaction and the cross reaction are not. Steric effects on the self-exchange and cross reactions can be quite different. More generally, organic reactions often involve an electrophile and a nucleophile so that self-reactions do not provide good insight into the kinetic barriers. HAT reactions that have such “polar effects” are known,¹⁵ and these will likely not follow the cross relation.

The accuracy of the simple Marcus model is also surprising because it ignores many of the insights of modern theories of proton-coupled electron transfer.³⁸ These theories suggest that many HAT reactions are electronically and vibrationally nonadiabatic and involve substantial proton tunneling. The modern theories do not simply reduce to the cross relation, so there is little²⁰ theoretical basis for its application. It should be emphasized that we have defined “success” of the cross relation as agreement to within ca. an order of magnitude. The more sophisticated treatments are clearly necessary to analyze the finer details of reactivity, such as kinetic isotope effects and their temperature dependence.

The success of the cross relation indicates that HAT rate constants are primarily determined by two parameters: the free energy of reaction (ΔG°) and the intrinsic barriers λ . The ΔG° is for transfer of H[•], so the reactions appear to involve relatively synchronous transfer of e⁻ and H[•]. If, for instance, the electron were to “go first” such that the transition structure involved much more ET than PT, deviations from the cross relation would be expected and rate constants might correlate better with E° 's than with BDFEs. The factors that influence λ are less understood, but it appears that much of the intuition from PT and ET applies to HAT. Reagents that have large intrinsic barriers to PT, such as C–H bonds, or large λ_{ET} , such as high-spin Co^{II}/low-spin Co^{III} couples, also have large λ_{HAT} . In sum, ΔG° , λ , and the cross relation provide a conceptual and predictive model for a wide range of HAT reactions.

Ongoing work is exploring the application of these ideas to reactions in which the H⁺ and e⁻ are quite separated, as in reaction 7 above.

The author is indebted to the many students, postdoctoral fellows, colleagues, and collaborators who have been an integral part of this work. He gratefully acknowledges the support of the U.S. National Institutes of Health (GM50422) and the University of Washington Department of Chemistry for their financial support.

BIOGRAPHICAL INFORMATION

James Mayer was born in New York City and did undergraduate research at Hunter College with Edwin Abbott, and with William Klemperer while earning his A.B. at Harvard. He completed a Ph.D. at Caltech under the direction of John Bercaw in 1982, and after two years as a Visiting Scientist at DuPont moved to the University of Washington, where he is now Alvin L. and Verla R. Kwiram Professor of Chemistry. His interests in redox chemical reactions span inorganic, organometallic, bioinorganic, and physical organic chemistry.

FOOTNOTES

*E-mail: mayer@chem.washington.edu.

REFERENCES

- (a) Kochi, J. K., Ed. *Free Radicals*; Wiley: New York, 1973. (b) Halliwell, B.; Gutteridge, J. M. C. *Free Radicals in Biology and Medicine*; Oxford University Press: Oxford, U.K., 2007.
- Mayer, J. M. Proton-Coupled Electron Transfer: A Reaction Chemist's View. *Annu. Rev. Phys. Chem.* **2004**, *55*, 363–390.
- Huynh, M. H. V.; Meyer, T. J. Proton-Coupled Electron Transfer. *Chem. Rev.* **2007**, *107*, 5004–5064.
- (a) Bryant, J. R.; Mayer, J. M. Oxidation of C–H Bonds by [(bpy)₂(py)Ru^{IV}(O)]²⁺ Occurs by Hydrogen Atom Abstraction. *J. Am. Chem. Soc.* **2003**, *125*, 10351–10361. (b) Bryant, J. R.; Matsuo, T.; Mayer, J. M. Cumene Oxidation by *cis*-[Ru^{IV}(bpy)₂(py)(O)]²⁺, Revisited. *Inorg. Chem.* **2004**, *43*, 1587–1592.
- Roth, J. P.; Mayer, J. M. Hydrogen Transfer Reactivity of a Ferric Bi-imidazole Complex That Models the Activity of Lipoxygenase Enzymes. *Inorg. Chem.* **1999**, *38*, 2760–2761.
- Waidmann, C. R.; Zhou, X.; Tsai, E. A.; Kaminsky, W.; Hrovat, D. A.; Borden, W. T.; Mayer, J. M. Slow Hydrogen Atom Transfer Reactions of Oxo- and Hydroxo-Vanadium Compounds: The Importance of Intrinsic Barriers. *J. Am. Chem. Soc.* **2009**, *131*, 4729–4743.
- Manner, V. W.; Mayer, J. M. Concerted Proton-Electron Transfer in a Ruthenium Terpyridyl-Benzoate System with a Large Separation between the Redox and Basic Sites. *J. Am. Chem. Soc.* **2009**, *131*, 9874–9875.
- Warren, J. J.; Tronic, T. A.; Mayer, J. M. The Thermochemistry of Proton-Coupled Electron Transfer Reactions and its Implications. *Chem. Rev.*, ASAP (DOI: 10.1021/cr100085k).
- Costentin, C.; Evans, D. H.; Robert, M.; Savéant, J.-M. Electrochemical Approach to Concerted Proton and Electron Transfers. Reduction of the Water-Superoxide Ion Complex. *J. Am. Chem. Soc.* **2005**, *127*, 12490–12491.
- Evans, M. G.; Polanyi, M. Inertia and Driving Force of Chemical Reactions. *Trans. Faraday Soc.* **1938**, *34*, 11–24.
- Matsuo, T.; Mayer, J. M. Oxidations of NADH Analogues by *cis*-[Ru^{IV}(bpy)₂(py)(O)]²⁺ Occur by Hydrogen-Atom Transfer Rather than by Hydride Transfer. *Inorg. Chem.* **2005**, *44*, 2150–2157.
- Shaik, S. S.; Schlegel, H. B.; Wolfe, S. *Theoretical Aspects of Physical Organic Chemistry: The S_N2 Mechanism*; Wiley: New York, 1992.
- Mayer, J. M.; Mader, E. A.; Roth, J. P.; Bryant, J. R.; Matsuo, T.; Dehestani, A.; Bales, B. C.; Watson, E. J.; Osako, T.; Valliant-Saunders, K.; Lam, W. H.; Hrovat,

- D. A.; Borden, W. T.; Davidson, E. R. Stoichiometric Oxidations of σ -Bonds: Radical and Possible Non-Radical Pathways. *J. Mol. Catal. A: Chem.* **2006**, *251*, 24–33.
- 14 R uchardt, C.; Gerst, M.; Ebenhoch, J. Uncatalyzed Transfer Hydrogenation and Transfer Hydrogenolysis: Two Novel Types of Hydrogen-Transfer Reactions. *Angew. Chem., Int. Ed. Engl.* **1997**, *36*, 1406–1430.
- 15 Tedder, J. M. Which Factors Determine the Reactivity and Regioselectivity of Free Radical Substitution and Addition Reactions. *Angew. Chem., Int. Ed. Engl.* **1982**, *21*, 401–410.
- 16 Roth, J. P.; Yoder, J. C.; Won, T.-J.; Mayer, J. M. Application of the Marcus Cross Relation to Hydrogen Atom Transfer Reactions. *Science* **2001**, *294*, 2524–2526.
- 17 Tsentelovich, Y. P.; Kulik, L. V.; Gritsan, N. P.; Yurkovskaya, A. V. Solvent Effect on the Rate of β -Scission of the *tert*-Butoxyl Radical. *J. Phys. Chem. A* **1998**, *102*, 7975–7980.
- 18 Sutin, N. Theory of Electron Transfer Reactions: Insights and Hintsights. *Prog. Inorg. Chem.* **1983**, *30*, 441–498.
- 19 See references in ref 2.
- 20 (a) Cohen, A. O.; Marcus, R. A. On the Slope of Free Energy Plots in Chemical Kinetics. *J. Phys. Chem.* **1968**, *72*, 4249–4256. (b) Marcus, R. A. H and Other Transfers in Enzymes and in Solution: Theory and Computations, a Unified View. 2. Applications to Experiment and Computations. *J. Phys. Chem. B* **2007**, *111*, 6643–6654.
- 21 Wu, A.; Mayer, J. M. Hydrogen Atom Transfer Reactions of a Ruthenium Imidazole Complex: Hydrogen Tunneling and the Applicability of the Marcus Cross Relation. *J. Am. Chem. Soc.* **2008**, *130*, 14745–14754.
- 22 Griller, D.; Ingold, K. U. Abstraction of the hydroxylic hydrogen of alcohols by alkoxy radicals. *J. Am. Chem. Soc.* **1974**, *96*, 630–632.
- 23 Chenier, J. H. B.; Howard, J. A. A Kinetic Electron Spin Resonance Study of the Transfer of a Hydrogen Atom from α -Tetralin Hydroperoxide to a Tertiary Alkylperoxy Radical. *Can. J. Chem.* **1975**, *53*, 623–627.
- 24 Jackson, R. A.; O'Neill, D. W. The Reaction of Benzyl Radicals with *m*-Deuteriotoluene. *J. Chem. Soc., Chem. Commun.* **1969**, 1210–1211.
- 25 Isborn, C.; Hrovat, D. A.; Borden, W. T.; Mayer, J. M.; Carpenter, B. K. Factors Controlling the Barriers to Degenerate Hydrogen Atom Transfers. *J. Am. Chem. Soc.* **2005**, *127*, 5794–5795, and references therein.
- 26 Wagner, P. J.; Zhang, Y.; Puchalski, A. E. Rate constants for degenerate hydrogen atom exchange between α -hydroxy radicals and ketones. *J. Phys. Chem.* **1993**, *97*, 13368–13374.
- 27 Shaik, S.; Kumar, D.; de Visser, S. P.; Altun, A.; Thiel, W. Theoretical Perspective on the Structure and Mechanism of Cytochrome P450 Enzymes. *Chem. Rev.* **2005**, *105*, 2279–2328.
- 28 Yoder, J. C.; Roth, J. P.; Gussenhoven, E. M.; Larsen, A. S.; Mayer, J. M. Electron and Hydrogen-Atom Self-Exchange Reactions of Iron and Cobalt Coordination Complexes. *J. Am. Chem. Soc.* **2003**, *125*, 2629–2640.
- 29 Xue, G. Q.; De Hont, R.; Munck, E.; Que, L., Jr. Million-fold activation of the $[\text{Fe}_2(\mu\text{-O})_2]$ diamond core for C-H bond cleavage. *Nat. Chem.* **2010**, *2*, 400–405.
- 30 Mader, E. A.; Larsen, A. S.; Mayer, J. M. Hydrogen Atom Transfer from Iron(II)-Tris[2,2'-bi(tetrahydropyrimidine)] to TEMPO: A Negative Enthalpy of Activation Predicted by the Marcus Equation. *J. Am. Chem. Soc.* **2004**, *126*, 8066–8067.
- 31 Marcus, R. A.; Sutin, N. Electron-transfer reactions with unusual activation parameters. Treatment of reactions accompanied by large entropy decreases. *Inorg. Chem.* **1975**, *14*, 213–216.
- 32 Mader, E. A.; Davidson, E. R.; Mayer, J. M. Large Ground-State Entropy Changes for Hydrogen Atom Transfer Reactions of Iron Complexes. *J. Am. Chem. Soc.* **2007**, *129*, 5153–5166.
- 33 Mader, E. A.; Manner, V. W.; Markle, T. F.; Wu, A.; Franz, J. A.; Mayer, J. M. Trends in Ground-State Entropies for Transition Metal Based Hydrogen Atom Transfer Reactions. *J. Am. Chem. Soc.* **2009**, *131*, 4335–4345.
- 34 cf. (a) Eckert, N. A.; Vaddadi, S.; Stoian, S.; Lachicotte, R. J.; Cundari, T. R.; Holland, P. L. Coordination-Number Dependence of Reactivity in an Imidoiron(III) Complex. *Angew. Chem., Int. Ed.* **2009**, *48*, 6868–6871. (b) Gunay, A.; Theopold, K. H. C-H Bond Activations by Metal Oxo Compounds. *Chem. Rev.* **2010**, *110*, 1060–1081. (c) England, J.; Martinho, M.; Farquhar, E. R.; Frisch, J. R.; Bominaar, E. L.; Munck, E.; Que, L. A Synthetic High-Spin Oxoiron(IV) Complex: Generation, Spectroscopic Characterization, and Reactivity. *Angew. Chem., Int. Ed.* **2009**, *48*, 3622–3626.
- 35 Mader, E. A.; Mayer, J. M. The Importance of Precursor and Successor Complex Formation in a Bimolecular Proton-Electron Transfer Reaction. *Inorg. Chem.* **2010**, *49*, 3685–3687.
- 36 Soper, J. D.; Kaminsky, W.; Mayer, J. M. Slow Hydrogen Atom Self-Exchange between Os(IV) Anilide and Os(III) Aniline Complexes: Relationships with Electron and Proton Transfer Self-Exchange. *J. Am. Chem. Soc.* **2003**, *125*, 12217–12229.
- 37 Wu, A.; Mader, E. A.; Datta, A.; Hrovat, D. A.; Borden, W. T.; Mayer, J. M. Nitroxyl Radical Plus Hydroxylamine Pseudo Self-Exchange Reactions: Tunneling in Hydrogen Atom Transfer. *J. Am. Chem. Soc.* **2009**, *131*, 11985–11997.
- 38 Hammes-Schiffer, S. Theory of Proton-Coupled Electron Transfer in Energy Conversion Processes. *Acc. Chem. Res.* **2009**, *42*, 1881–1889.
- 39 Litwinienko, G.; Ingold, K. U. Solvent Effects on the Rates and Mechanisms of Reaction of Phenols with Free Radicals. *Acc. Chem. Res.* **2007**, *40*, 222–230.
- 40 Abraham, M. H.; Grellier, P. L.; Prior, D. V.; Morris, J. J.; Taylor, P. J. Hydrogen Bonding. Part 10. A Scale of Solute Hydrogen-bond Basicity Using log *K* Values for Complexation in Tetrachloromethane. *J. Chem. Soc., Perkin Trans. 2* **1990**, 521–529.
- 41 Warren, J. J.; Mayer, J. M. Predicting Organic Hydrogen Atom Transfer Rate Constants Using the Marcus Cross Relation. *Proc. Natl. Acad. Sci. U.S.A.* **2010**, *107*, 5282–5287.
- 42 Mayer, J. M.; Hrovat, D. A.; Thomas, J. L.; Borden, W. T. Proton-Coupled Electron Transfer versus Hydrogen Atom Transfer in Benzyl/Toluene, Methoxyl/Methanol, and Phenoxyl/Phenol Self-Exchange Reactions. *J. Am. Chem. Soc.* **2002**, *124*, 11142–11147.